The International Journal of Advanced Manufacturing Technology (2018) 97:1149–1163
https://doi.org/10.1007/s00170-018-1982-1

ORIGINAL ARTICLE

A region-based 3 + 2-axis machining toolpath generation method for freeform surface

Xu Liu[1] · Yingguang Li[2] · Qiang Li[2]

Received: 9 September 2017 / Accepted: 2 April 2018 / Published online: 20 April 2018
© Springer-Verlag London Ltd., part of Springer Nature 2018

Abstract
Due to the geometric complexity, tool orientations usually change dynamically during freeform surface machining with 5-axis machine tool. As the kinematic performance of the rotary axes is usually weaker than that of the linear axes, the real cutting speed is difficult or even impossible to reach the desired level, which further leads to low machining efficiency. This paper presents a region-based 3 + 2-axis machining toolpath generation method with 5-axis machine tool. The surface is first divided into several preliminary sub-surfaces using K-means clustering algorithm. A post processing procedure is then carried out to optimise the preliminary sub-surfaces to ensure the machinability. For each sub-surface, gouging-/collision-free tool orientations are first calculated and then the optimal combination of the fixed tool orientation and the feed direction is determined by maximising the average machining strip width for toolpath generation. The proposed method is tested by a case surface and the comparisons to some other traditional methods are also provided.

Keywords NC machining · Freeform surface · 3 + 2-axis machining · Surface subdivision · Toolpath generation

1 Introduction

Nowadays, 5-axis machine tools are widely applied to machine freeform surface parts in industries like automotive, aerospace and energy. Compared to 3-axis machines, the two additional rotary axes of 5-axis machines greatly increase the accessibility and flexibility of machining [1, 2]. As a result, a closer match of the cutter's shape to the surface could be achieved which means larger machining strip width (MSW) and shorter toolpath length. Ball end mills now are not the only choice for cutting freeform surfaces which will significantly improve the surface quality as well as the machining efficiency.

However, due to the geometric complexity, tool orientations usually change dynamically during freeform surface machining with 5-axis machine tool. As the kinematic performance (velocity, acceleration and jerk) of the rotary axes is usually weaker than that of the linear axes, the real cutting speed is difficult or even impossible to reach the desired level, which further results in bad machining efficiency. Great efforts have been made to reduce the 5-axis machining time of freeform surfaces by tool orientation smoothing and MSW optimisation [3, 4]. Another effective idea is 3 + 2-axis machining which is in between 3-axis and 5-axis machining. It is to use the 5-axis capability to orient the cutter and fix this tool orientation during the machining to obtain an optimal real cutting speed. Recent progresses on these three research aspects are as follows.

1.1 Tool orientation smoothing

Tool orientation smoothing is to find the optimal smoothly varying gouge-free orientations at cutter contact points (CCP) to enlarge the real cutting speed. Tool orientations without local gouging, rear gouging and global collision are usually represented in various ways which further result in different smoothing procedures. Jun et al. [5] eliminated the dramatic changes of tool orientations by identifying the shortest distance in a 2D configuration space (C-space). Later in the research of Lu et al. [6], the height of the cutter lifted along the normal of the surface was defined as the third variable to establish a 3D C-space. Tool orientations were smoothed by searching the available C-space set with the minimum motion time distance to the ideal C-space set for each CCP. Wang and

✉ Yingguang Li
liyingguang@nuaa.edu.cn

[1] School of Mechanical and Power Engineering, Nanjing Tech University, Nanjing 210009, China

[2] College of Mechanical and Electrical Engineering, Nanjing University of Aeronautics and Astronautics, Nanjing 210016, China

Tang [7] generated the feasible tool orientations of each CCP by constructing the visibility map VMap. Then partial and full backward retractions were applied by considering the angular velocity limit to avoid quick changes in tool orientations between neighbouring CCPs. The concept of the domain of admissible orientation (DAO) was proposed by Castagnetti et al. [8] to restrict the possible orientations of the tool axis for each CCP. Both the angular difference between two successive points and the curvature of the evolution were minimised based on the DAO constructed in the machine coordinate system. To ensure a constant speed of the tool cutting edge against the surface, Farouki and Li [9] defined the possible tool orientations at each CCP as a cone of angle ψ about its surface normal. Smoothing method based on parallel transport of the tangent component of the tool orientation was then proposed for rotation-minimising tool orientations.

1.2 MSW optimisation

To improve the machining efficiency, another effective way is to reduce the total toolpath length by maximising the MSW at each CCP. Effective cutting shape (ECS) is usually defined as the approximation of the cutter surface [10]. MSW can be enlarged by increasing the proximity of the surface normal curvature and the ECS curvature. The traditional idea is generating the optimal toolpaths by considering the whole surface as one machining region. Fard and Feng [11] indicated that if the cutter moves along the minimum curvature direction, the MSW could be increased, especially for freeform surfaces with low-curvature relative to the cutter size. In Gong et al.'s research [12], MSW was optimised by minimising the relative normal curvature between the cutter envelope surface and the designed surface. However, for complex surface machining, toolpaths with maximal MSW usually present vary among different regions. Thus, to get global optimal machining results, region-based toolpaths may be required [13]. Chiou and Lee [14] established the concept of machining potential field for selecting the toolpath with the maximum average MSW among the potential paths across the surface as the start toolpath. During the generation of adjacent toolpaths, if the cutting efficiency of a newly generated adjacent toolpath falls below a predefined value, the procedure will stop and a new initial toolpath will be selected to continue the toolpath computation in the blank area of the surface. Anotaipaiboon and Makhanov [15] first constructed two isoparametric toolpaths along two parametric directions and then generated space-filling curves adaptively by following the directions with larger MSW. Thus, in different sub-surfaces, toolpaths follow different parametric directions. Liu et al. [16] developed a rank two tensor for evaluating the MSW. MSW tensor field was established to divide the surface into sub-surfaces by extracting the trisector degenerate points. In each sub-surface, feed directions for maximal MSW follow the same or similar pattern. As a result, toolpaths in each sub-surface can be generated separately for global optimal machining.

1.3 3 + 2-axis machining

3 + 2-axis machining uses the 5-axis capability to orient the cutter and fix this orientation during the machining. Apparently, this strategy can improve the real cutting speed especially for complex surface machining. However, it is usually difficult or even impossible to determine such a fixed tool orientation optimally. Gray et al. [17] proposed a tool positioning strategy named the arc-intersect method to optimise the tool orientation for given 3 + 2-axis machining toolpaths. Chen et al. [18] used fuzzy pattern clustering techniques and Voronoi diagram to divide the surface into several patches. Both toolpath and the set-up for each surface patch were planned for 3 + 2-axis machining. Roman et al. [19] classified the surface geometric properties into three categories, i.e. proximity parameters, orientation parameters and curvature parameters. Surface subdivision for 3 + 2-axis machining was then carried out by applying fuzzy C-means method with these parameters. Flores [20] provided the comparisons among different clustering algorithms for 3 + 2-axis machining for surface subdivision and introduced a detailed patch-by-patch machining method. Bi et al. [21] defined the accessibility cone of a mill cutter and used the GPU-based method to optimise the tool orientation and the safe cutter length for 3 + 2-axis machining. Zhu et al. [22] established a tool orientation planning method to maximise the average MSW for 3 + 2-axis machining by finding the quasi-feasible sector domain.

This paper introduces an improved region-based 3 + 2-axis machining toolpath generation method for freeform surfaces using 5-axis machine tool. Section 2 will show a detailed surface subdivision method. K-means clustering algorithm is applied to classify all surface points into several categories for preliminary surface subdivision. Different from existing methods, a post processing procedure is also put forward to optimise this subdivision result for ensuring the machinability. In Section 3, for each sub-surface, gouging-/collision-free tool orientations are first calculated and then the optimal combination of the fixed tool orientation and the feed direction is determined by maximising the average MSW of all CCPs to generate toolpaths. In Section 4, a case is provided to test the proposed method. Comparisons to some other traditional methods are also given. At last, Section 5 will conclude the whole paper and discuss the future work.

2 Surface subdivision for 3 + 2-axis machining

The proposed surface subdivision method has two procedures. Firstly, surface points will be classified into different categories by applying K-means clustering algorithm. Preliminary

sub-surfaces could be obtained by constructing the boundaries between adjacent point categories. Then, this surface subdivision result will be optimised by partitioning and merging the areas with bad machinability.

2.1 Surface subdivision based on K-means clustering

The surface is first meshed to extract discrete surface points. Then, the K-means clustering algorithm which is a classical algorithm in cluster analysis and usually requires shorter computing time to get similar result compared to other clustering methods is used to put the surface points into different clusters. The main procedure is shown in Fig. 1.

For each surface point $\boldsymbol{P}_i$, a multi-dimensional vector $\boldsymbol{V}_i$ is constructed by combining its position and normal vectors as

$$\boldsymbol{V}_{\mathrm{i}} = [\boldsymbol{P}_{\mathrm{i}} \ \ \boldsymbol{N}_{\mathrm{i}}] = \left[p_{\mathrm{ix}} \ p_{\mathrm{iy}} \ p_{\mathrm{iz}} \ n_{\mathrm{ix}} \ n_{\mathrm{iy}} \ n_{\mathrm{iz}}\right] \tag{1}$$

Normalise $\boldsymbol{V}_i$ by

$$\boldsymbol{F}_{\mathrm{i}} = \frac{\boldsymbol{V}_{\mathrm{i}} - \mathrm{Min}(\boldsymbol{V}_{\mathrm{i}})}{\mathrm{Max}(\boldsymbol{V}_{\mathrm{i}} - \mathrm{Min}(\boldsymbol{V}_{\mathrm{i}}))} \tag{2}$$

where Min() and Max() are the functions to search the minimal and maximal parameters. $\boldsymbol{F}_i$ is called the feature vector for $\boldsymbol{P}_i$. For all the surface points, a feature vector space could be obtained as

$$\mathbf{S} = \{\boldsymbol{F}_{\mathrm{i}} | \boldsymbol{F}_{\mathrm{i}}, \mathrm{i} = 1, 2, \ldots, n\} \tag{3}$$

where n is the number of the surface points.

In K-means clustering, "K" refers the desired number of clusters and is normally selected from $[1, \ \sqrt{n}]$. Once K is determined, a feature vector is randomly chosen from $\boldsymbol{S}$ as the initial centroid $\boldsymbol{C}_j$ for each cluster. For any of the rest feature vectors $\boldsymbol{F}_i$, the square-error distances to all centroids are calculated by

$$d_{\mathrm{ij}} = \left\| \boldsymbol{F}_{\mathrm{i}} - \boldsymbol{C}_{\mathrm{j}} \right\|^2, \mathrm{j} = 1, 2, \ldots \mathrm{K} \tag{4}$$

Associate $\boldsymbol{F}_i$ to the centroid that makes the minimal d_{ij}. Based on this way, all the feature vectors could be put into a cluster. Then, relocate every centroid by using the mean of the feature vectors belonging to the cluster. As a result, the square-error distances are updated and the feature vectors need to be associated to new centroids. This iterative process will continue until the centroids do not move. At this time, we should evaluate whether the number of clusters is advisable. Define normal

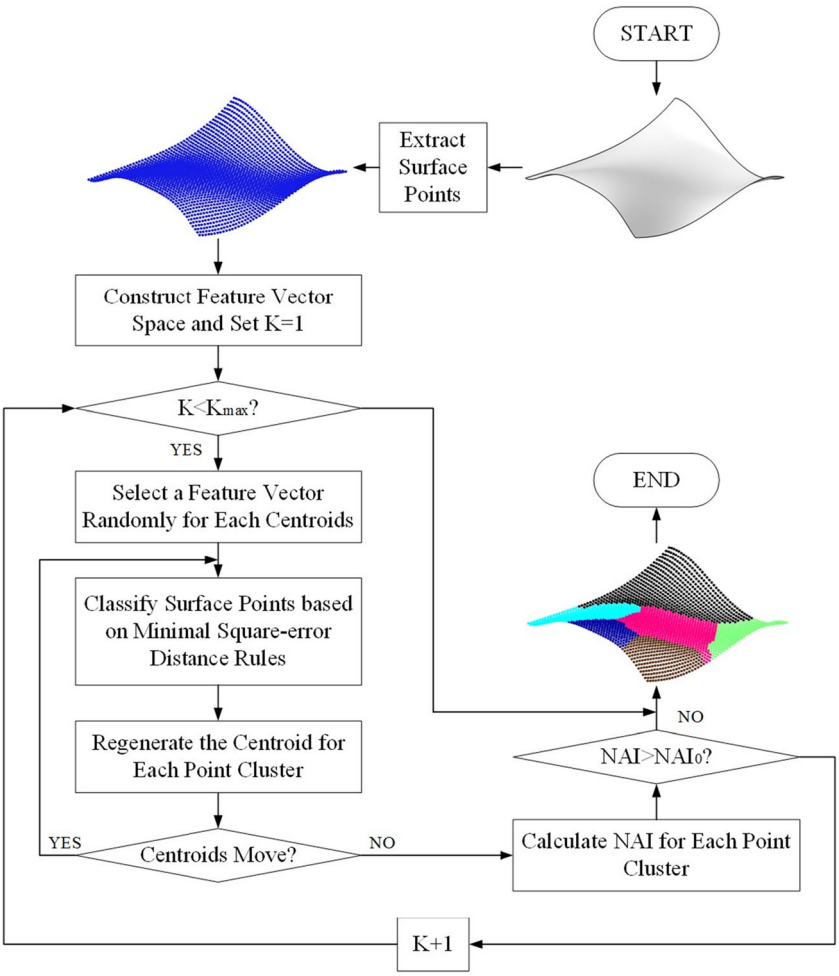

Fig. 1 Procedures of K-means clustering for surface point classification

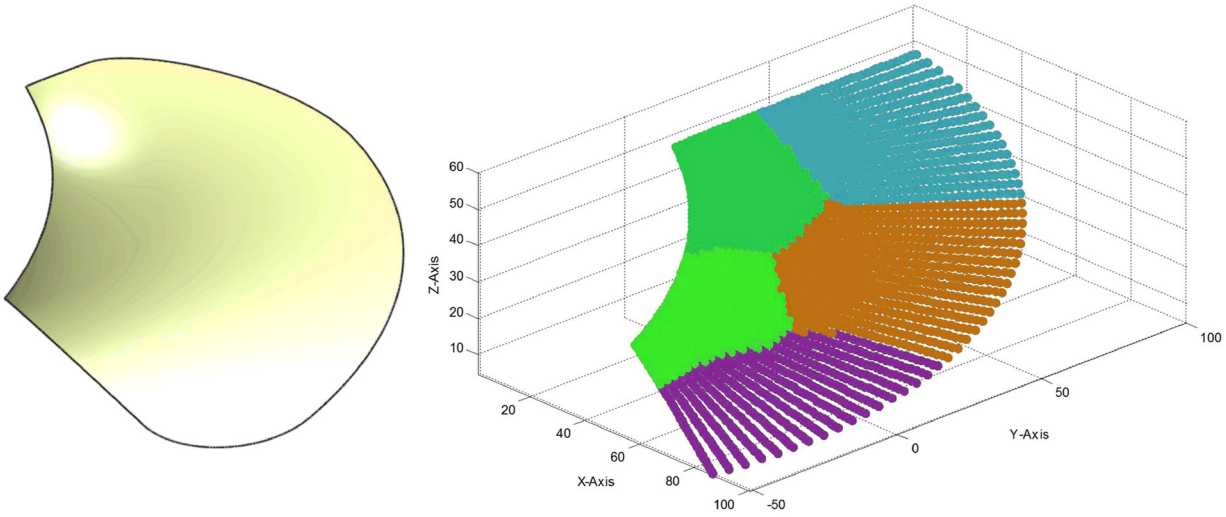

a. Surface Point Clusters of Blade Surface a

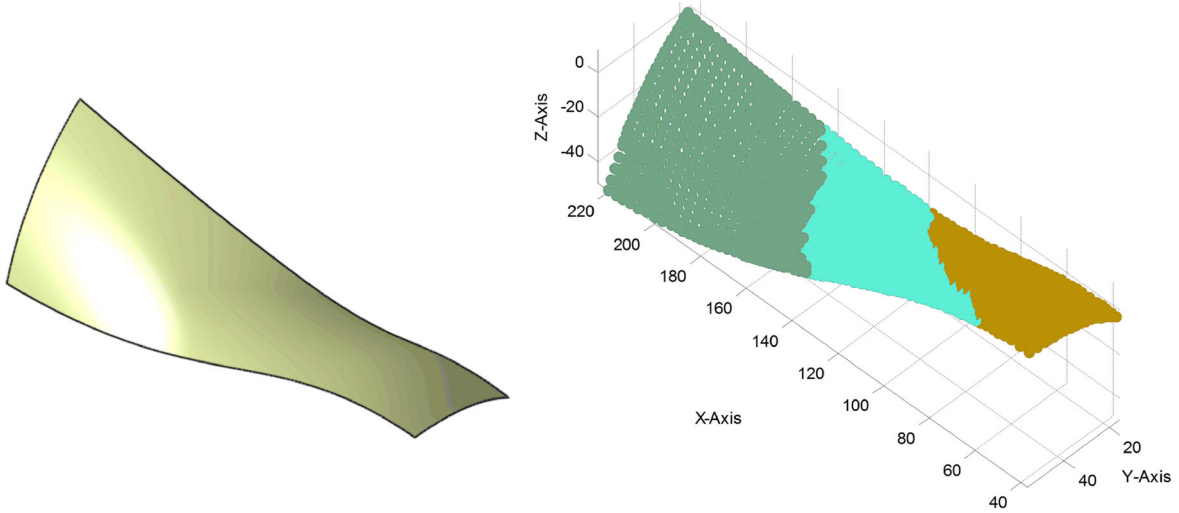

b. Surface Point Clusters of Blade Surface b

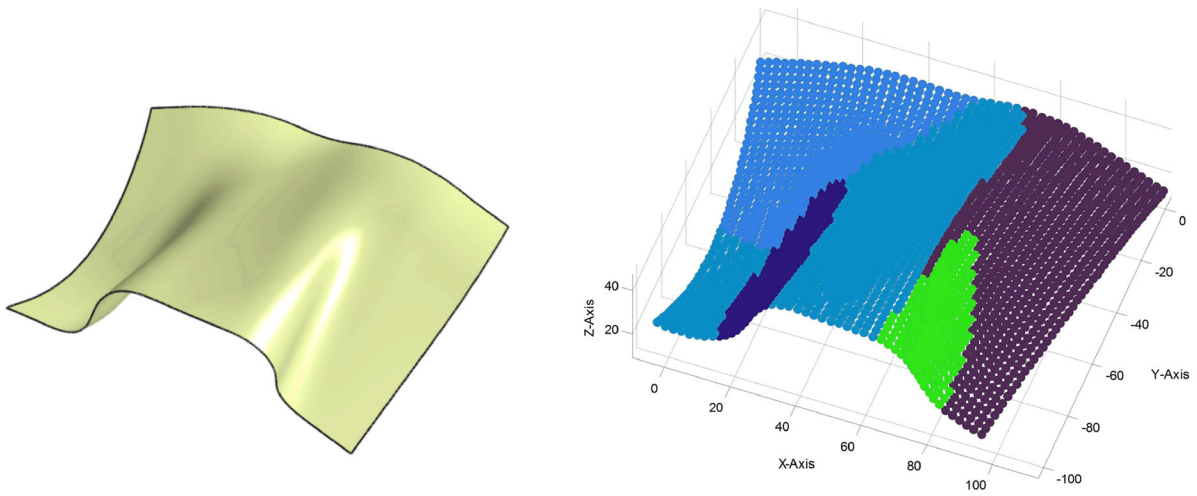

c. Surface Point Clusters of a Mold Surface

Fig. 2 Examples of surface point classification using K-means clustering

aggregation index (NAI) to represent the maximal angle between the normal vectors and the mean normal vector in each point cluster. If NAI > NAI_0, where NAI_0 is a predefined angle for measuring the similarity of the points inside a cluster, K should be plus 1 and the clustering procedures should be rerun with the new K. With the above method, surface points could be classified into different categories. Three examples are shown in Fig. 2.

After getting the point clusters, boundaries could be constructed within the surface for acquiring sub-surfaces. Apparently, the sawtooth-shaped boundaries by connecting the boundary points cannot be directly used not only for the bad surface machining quality but also for the inconsideration to the areas between adjacent point clusters. To generate inside boundaries, we should first extract all boundary grids (BG) that contain points from at least two clusters. BGs could be classified into four classes:

a. Cross boundary grids (CBG): the BGs whose points are shared by more than two clusters as shown in Fig. 3a. CBGs contain the intersections of inside boundaries.
b. Outside boundary grids (OBG), the BGs include points on the outside boundaries of the surface, as shown in Fig. 3b.
c. Corner boundary grids (CoBG): the BGs are made up of one point from a cluster and three from the other, as shown in Fig. 3c.
d. Normal boundary grids (NBG): the BGs except the upper three classes.

Both CBG and OBG are defined as extreme grid (EG). Furthermore, the centres of CBGs and the grid boundaries of OBGs shared by the surface are named as extreme points (EP). The BGs now could be divided into BG groups and each of

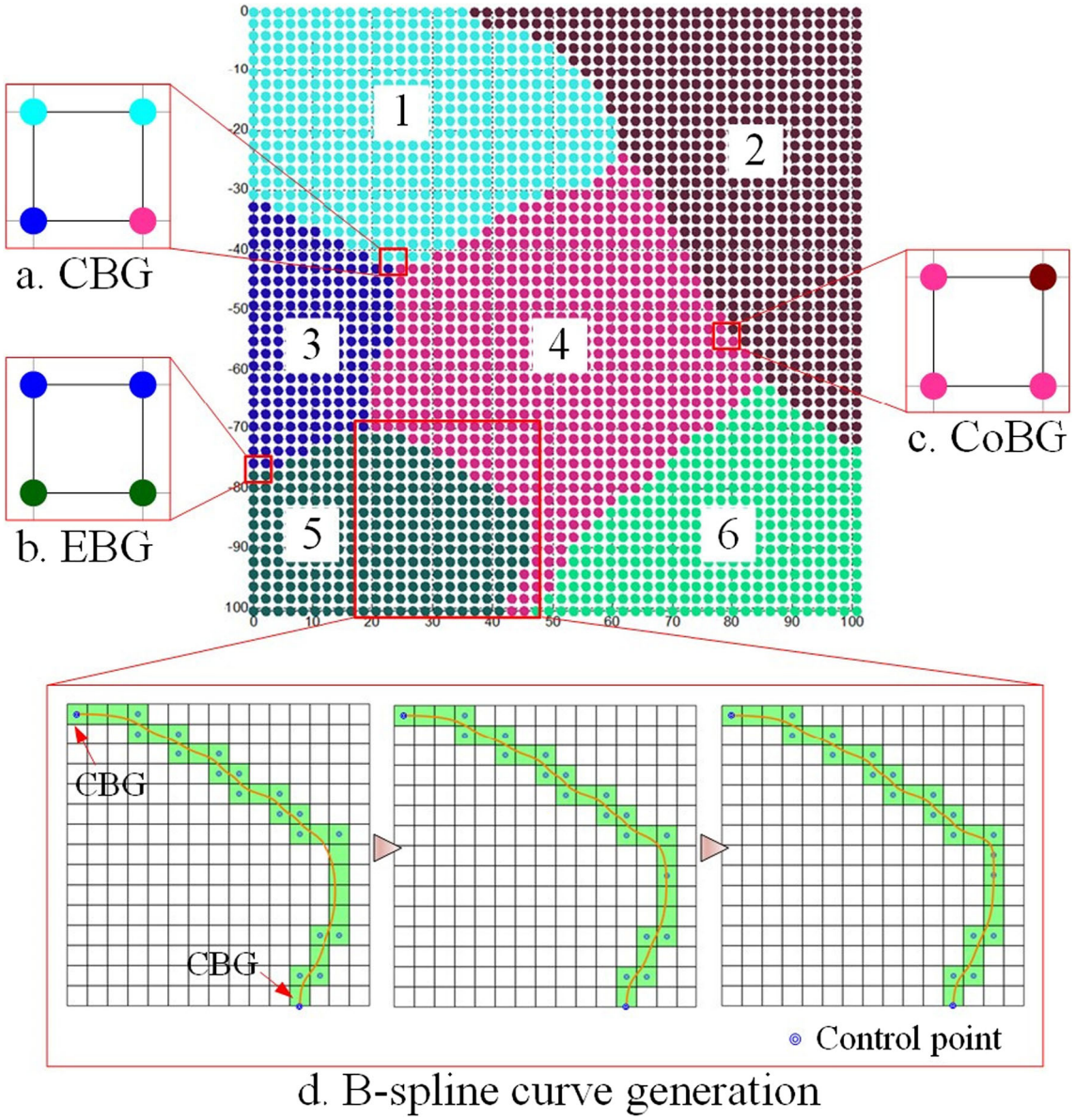

Fig. 3 Boundary construction

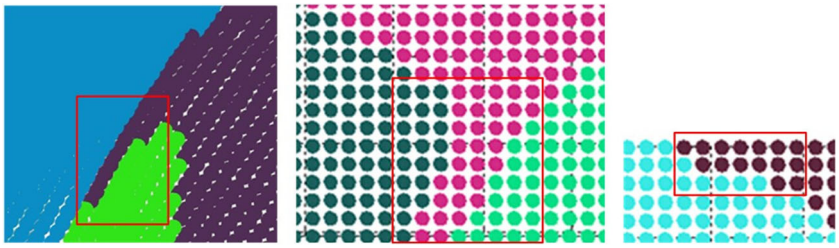

Fig. 4 Areas with poor machinability

them is made up of two EGs and the BGs between them. For each BG group, the EPs as well as the centres of CoBGs are used as control points for constructing B-spline curve as the inside boundary. If the spline curve exceeds the space restricted by the BG group, add the centres of the NBGs between the CoBGs nearby to the control point list as shown in Fig. 3d.

2.2 Sub-surfaces post processing

After the above procedures, the surface may be divided into several sub-surfaces. However, due to the geometric complexity, there are usually some areas with poor machinability so-called non-machining regions as shown in Fig. 4. When machining these narrow areas, the cutter may have to approach and retract frequently which will lead to low machining efficiency. Furthermore, serious cutting marks will be left on the surface to reduce the surface quality. In this paper, this kind of areas will be extracted and merged into other adjacent sub-surfaces.

To find non-machining regions, configuration-space (C-space) method is applied. For each sub-surface, project its boundary curves onto the perpendicular plane of the mean normal vector as bottom boundaries (BB). Offset BBs inwards by r where r is the cutter radius. The regions defined by the offset boundaries (OB) in which the minimal distance between OBs and BBs is no less than D/2 are called machining C-space

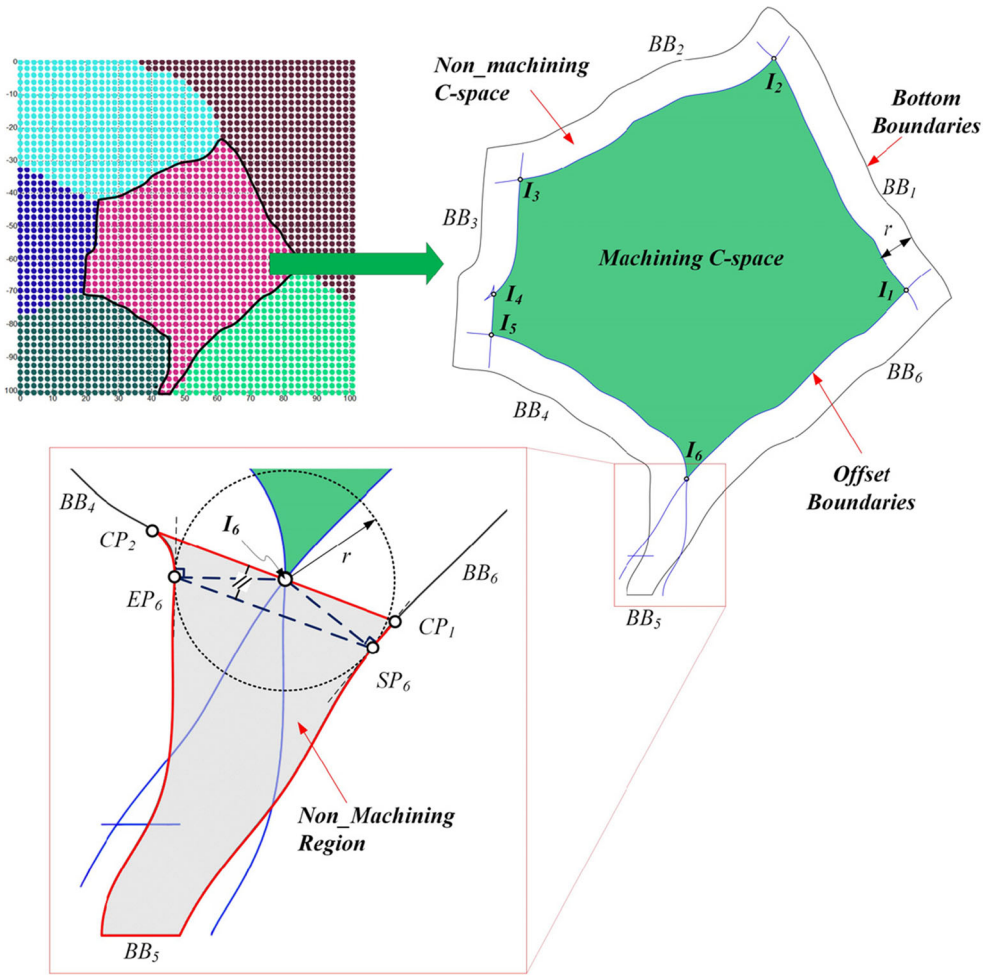

Fig. 5 Non-machining region generation

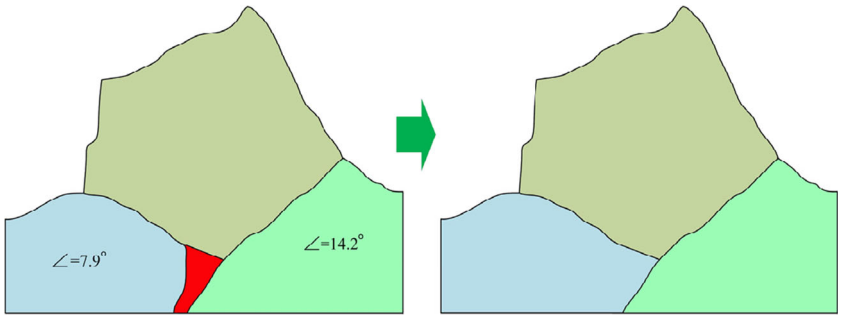

Fig. 6 Non-machining region merging

as shown in Fig. 5. The rest space in the region defined by BBs is called non-machining C-space. For each vertex of the machining C-spaces, construct a circle with diameter D. When the circle intersects the BBs at two points, calculate their distance. If it is larger than L_0 which is a predefined threshold, construct a straight line parallel to the vector passing the two intersections across the vertex. The region defined by this line and BBs in the non-machining C-space is the non-machining region as the shaded area shown in Fig. 5. The non-machining regions need to be merged into proper adjacent sub-surfaces. For each non-machining region, calculate the angles between its mean normal vector and the mean normal vectors of other adjacent sub-surfaces. The non-machining region should be merged into the adjacent sub-surface which refers to the minimal angle, as the case shown in Fig. 6.

3 Toolpath generation for sub-surfaces

In the proposed method, 3 + 2-axis machining toolpaths are separately generated in each sub-surface. The first step is to find all feasible fixed tool orientations in each sub-surface. Then, to further improve the machining efficiency, the final tool orientation will be determined together with the feed direction for larger average MSW.

3.1 Feasible tool orientation generation

During 3 + 2-axis machining, the two rotary axes of the machine tool will be fixed until the machining of the current sub-surface is finished. To get this fixed tool orientation, all the feasible tool orientations (FTO) which are gouging and collision free should be extracted firstly. The available tool orientation (ATO) space of a machine tool is usually restricted by the motion limits of two rotary axes and is usually represented as part of a Gaussian sphere constructed in the workpiece coordinate system (WCS), as shown in Fig. 7. By meshing this partial Gaussian sphere with proper angle step, ATOs of each sub-surface can be represented as a vector group $\boldsymbol{T}$. With the procedures shown in Fig. 8, once an ATO causes either local gouging, rear gouging or global collisions will be deleted from $\boldsymbol{T}$ forever to reduce the evaluation space gradually for computing efficiency improving. The detailed evaluations to the ATOs are as follows:

3.1.1 Local gouging evaluation

Local gouging occurs due to the mismatch in local curvatures between the cutter surface and the part surface as shown in Fig. 8b. The selected cutter is first rotated to $\boldsymbol{T}_j$ and then

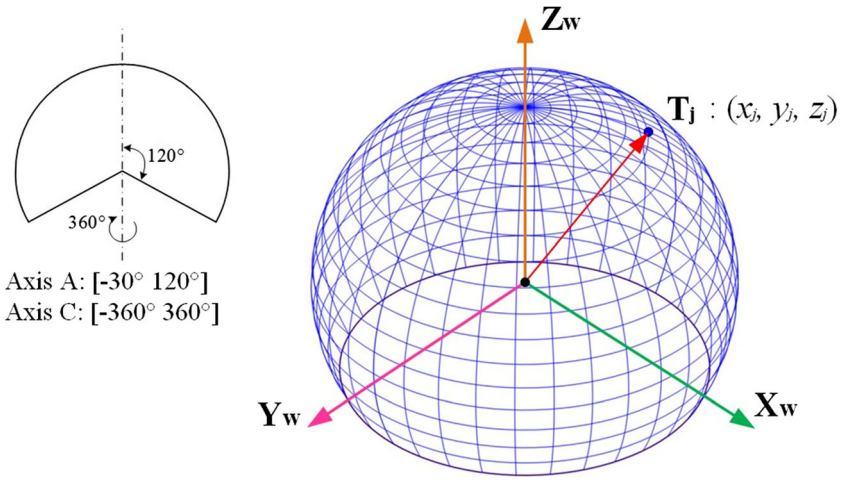

Fig. 7 ATO space of a machine tool defined on Gaussian sphere

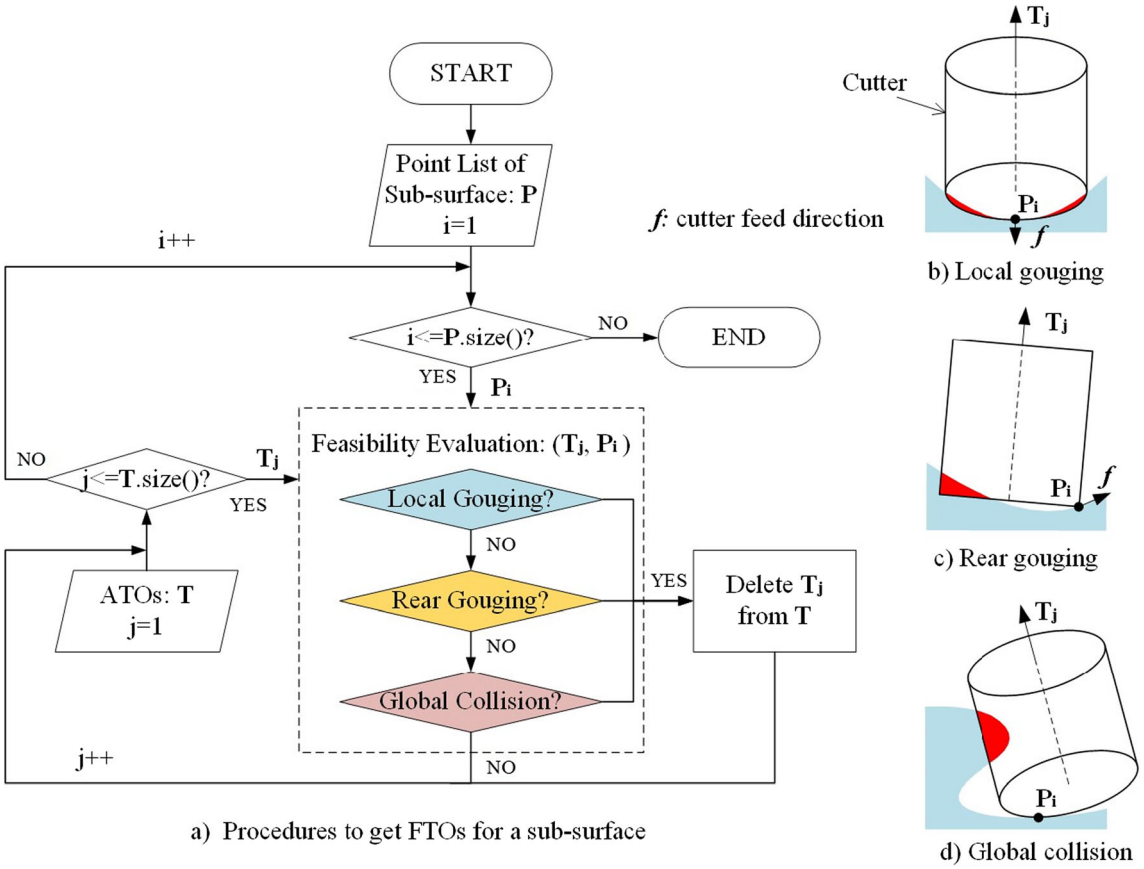

Fig. 8 Procedures to achieve FTOs. **a** Procedures to get FTOs for sub-surface. **b** Local gouging. **c** Rear gouging. **d** Global collision

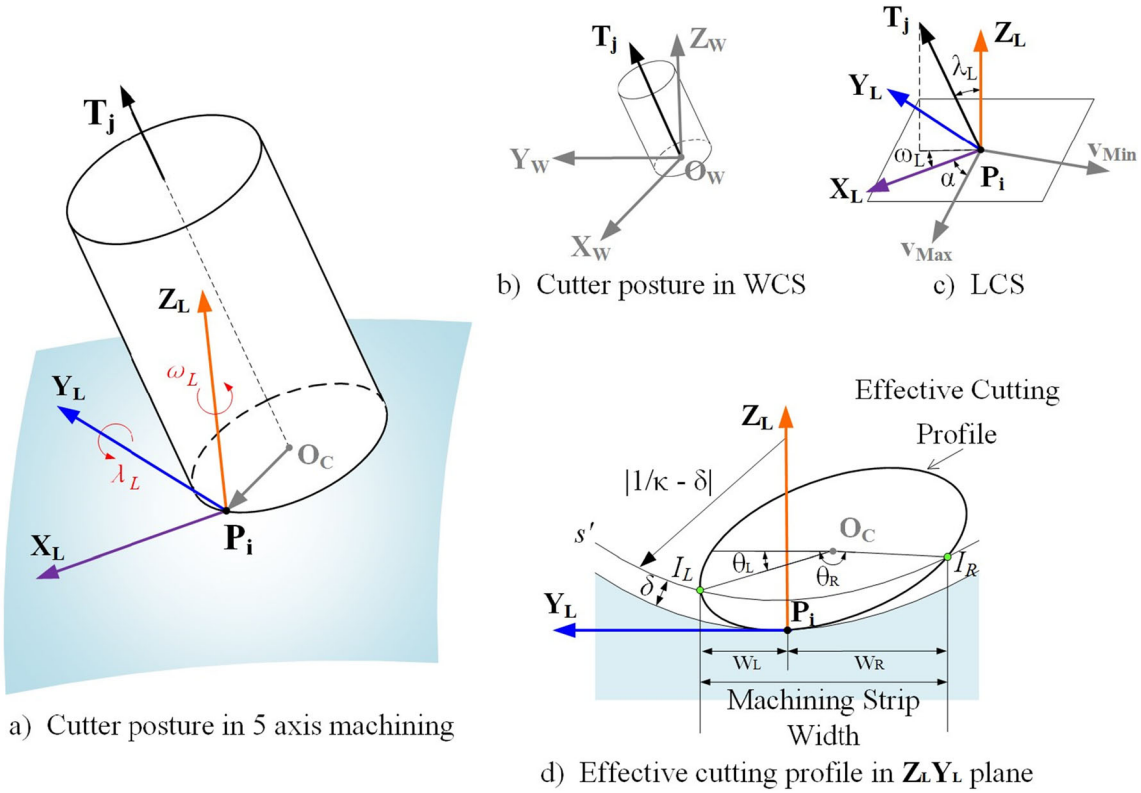

Fig. 9 Cutter with orientation T_j at P_i. **a** Cutter posture in 5-axis machining. **b** Cutter posture in WCS. **c** LCS. **d** Effective cutting profile in $Z_L Y_L$ plane

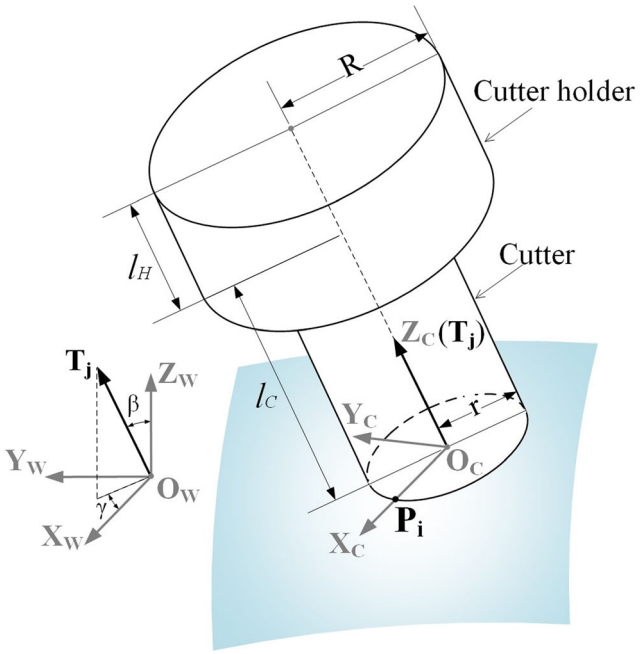

Fig. 10 Cutter coordinate system at $\boldsymbol{P}_i$

assigned to $\boldsymbol{P}_i$. The cutter centre $\boldsymbol{O}_C$ shown in Fig. 9a could be calculated by

$$\boldsymbol{O}_C = \boldsymbol{P}_i + \frac{\boldsymbol{T}_j \times (\boldsymbol{N}_i \times \boldsymbol{T}_j)}{|\boldsymbol{T}_j \times (\boldsymbol{N}_i \times \boldsymbol{T}_j)|} \cdot r \tag{5}$$

where $\boldsymbol{N}_i$ is the surface normal vector at $\boldsymbol{P}_i$ and r is the cutter radius. For each $\boldsymbol{P}_i$, a local coordinate system (LCS) could be established as shown in Fig. 9c. $\boldsymbol{X}_L$ is the instantaneous cutter feed direction. $\boldsymbol{Z}_L$ is the surface normal vector. $\boldsymbol{Y}_L$ is $\boldsymbol{X}_L \times \boldsymbol{Z}_L$. The surface curvature at $\boldsymbol{P}_i$ in $\boldsymbol{Y}_L\boldsymbol{Z}_L$ plane is

$$\kappa^{PS}_{Y_L Z_L} = \kappa_{min}\cos^2\alpha + \kappa_{max}\sin^2\alpha \tag{6}$$

where κ_{min} and κ_{max} are the principle curvatures at $\boldsymbol{P}_i$, α is the angle between $\boldsymbol{X}_L$ and the maximal principle direction $\boldsymbol{v}_{max}$ at $\boldsymbol{P}_i$. $\boldsymbol{T}_j$ defined in WCS could always be represented by a tilt angle λ_L and yaw angle ω_L in LCS, as shown in Fig. 9c. The projection of the cutter bottom on $\boldsymbol{Y}_L\boldsymbol{Z}_L$ plane is called effective cutting profile (ECP) as shown in Fig. 9d. The cutter surface curvature is the curvature of ECP at $\boldsymbol{P}_i$ and could be calculated by [23].

$$\kappa^{CS}_{Y_L Z_L} = \frac{\sin\lambda_L}{r\cos^2\omega_L} \tag{7}$$

At $\boldsymbol{P}_i$, the cutter could move along every tangent vector. Therefore, every α refers to a LCS. Since for given $\boldsymbol{P}_i$ and $\boldsymbol{T}_j$, ω_L is defined by the LCS, $\kappa^{CS}_{Y_L Z_L}$ also changes with α. Then, α leads to local gouging with $\boldsymbol{T}_j$ at $\boldsymbol{P}_i$ could be calculated by

$$\left\{\alpha \middle| \frac{\sin\lambda_L}{r\cos^2\omega_L(\alpha)} < \kappa_{min}\cos^2\alpha + \kappa_{max}\sin^2\alpha, \alpha\in[0, 2\pi]\right\} \tag{8}$$

In this paper, we choose a critical principle for local gouging avoidance that once the above set is not NULL, $\boldsymbol{T}_j$ will be deleted from $\boldsymbol{T}$. To increase the computing efficiency, points where both κ_{min} and κ_{max} are negative are skipped since no

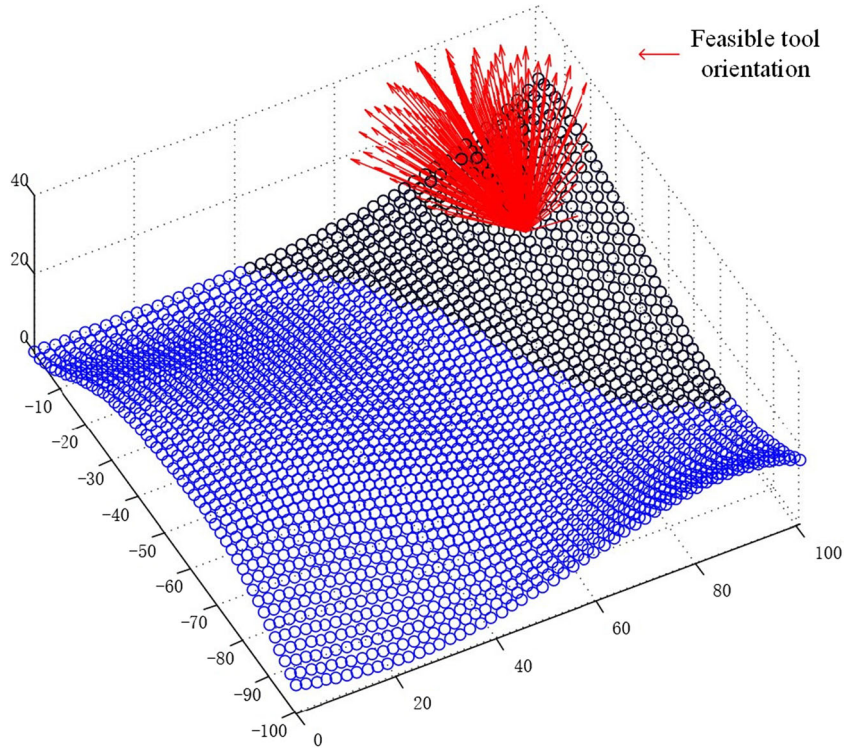

Fig. 11 FTOs for a sub-surface

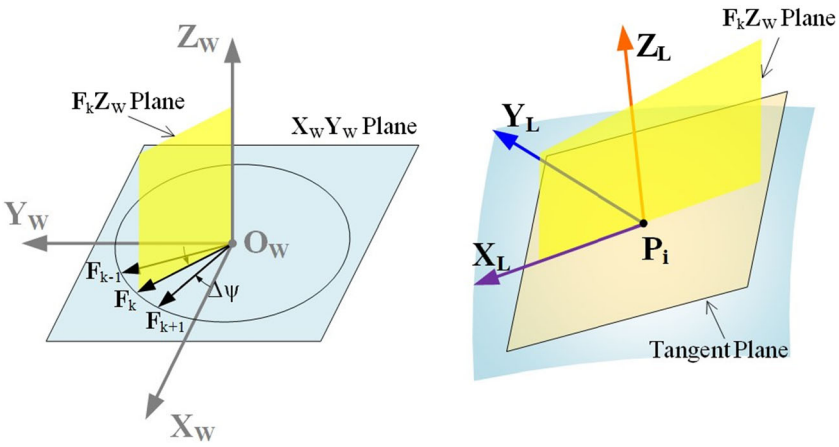

Fig. 12 X_L: the intersection of F_kZ_W plane and the tangent plane at P_i

local gouging will happen at convex positions. For the rest points, they should be evaluated in order, from the largest $\kappa_{\max}$ to the smallest $\kappa_{\max}$; thus, the infeasible ATO could be found at an early date.

3.1.2 Rear gouging and global collision evaluation

Rear gouging refers to the interference occurring between the cutter bottom and the part surface while global collision is the interference of the cylindrical part of the cutter or cutter holder and the part surface, as shown in Fig. 8c, d. When the cutter with orientation $\boldsymbol{T}_j$ was assigned to $\boldsymbol{P}_i$, a cutter coordinate system (OCS) could be established as shown in Fig. 10. The cutter centre O_C is the origin. $\boldsymbol{X}_C$ and $\boldsymbol{Z}_C$ are parallel to $\boldsymbol{O}_C\boldsymbol{P}_i$ and $\boldsymbol{T}_j$ respectively. $\boldsymbol{Y}_C$ is $\boldsymbol{X}_C \times \boldsymbol{Z}_C$. For rear gouging and global collision evaluation, surface points could be represented in OCS as

$$\boldsymbol{P}_{\mathrm{i}}^{\mathrm{C}} = {}_{W}^{C}\boldsymbol{R}\cdot\boldsymbol{P}_{\mathrm{i}} + \boldsymbol{O}_{\mathrm{C}} \tag{9}$$

where ${}_{W}^{C}\boldsymbol{R}$ is the rotation matrix

$${}_{W}^{C}\boldsymbol{R} = \mathrm{Rot}(\boldsymbol{Y}_{\mathrm{W}}, \beta)\mathrm{Rot}(\boldsymbol{Z}_{\mathrm{W}}, \gamma) \tag{10}$$

β and γ are angles between $\boldsymbol{T}_j$ and $\boldsymbol{Z}_W$, $\boldsymbol{X}_W$ as shown in Fig. 10. In this paper, the cutter holder is simplified as a cylinder with radius R and length l_H. $\boldsymbol{P}_i^C$ is a rear gouging or global collision point if the following equations are satisfied

$$\begin{cases} x_{\boldsymbol{P}_i^C}^2 + y_{\boldsymbol{P}_i^C}^2 \le r^2, \text{ when } z_{\boldsymbol{P}_i^C} \in [0, l_C] \\ x_{\boldsymbol{P}_i^C}^2 + y_{\boldsymbol{P}_i^C}^2 \le R^2, \text{ when } z_{\boldsymbol{P}_i^C} \in [l_C, l_H] \end{cases} \tag{11}$$

Similar to local gouging evaluation, once a surface point is found on or inside the cutter and cutter holder, $\boldsymbol{T}_j$ will be regarded as infeasible and deleted from $\boldsymbol{T}$.

Surface in Fig. 3 is tested using the above FTO generation method. The machine tool is Mikron UCP710. The rotation limits of axis A and C are [− 30° 120°] and [− 360° 360°] respectively. The cutter radius is 5 mm, the cutter length (outside the cutter holder) is 40 mm, the cutter holder radius is 20 mm and the cutter holder length is 30 mm. The FTOs of region 2 is shown in Fig. 11.

3.2 Toolpath generation

Toolpaths for machining a sub-surface using 3 + 2-axis strategy in this paper are parallel lines when projected to the $\boldsymbol{X}_W\boldsymbol{Y}_W$ plane for easy computation. Therefore, the first task for sub-surface toolpaths generation is to decide a cutter feed direction and tool orientation. Firstly, possible cutter feed directions $\boldsymbol{F}$

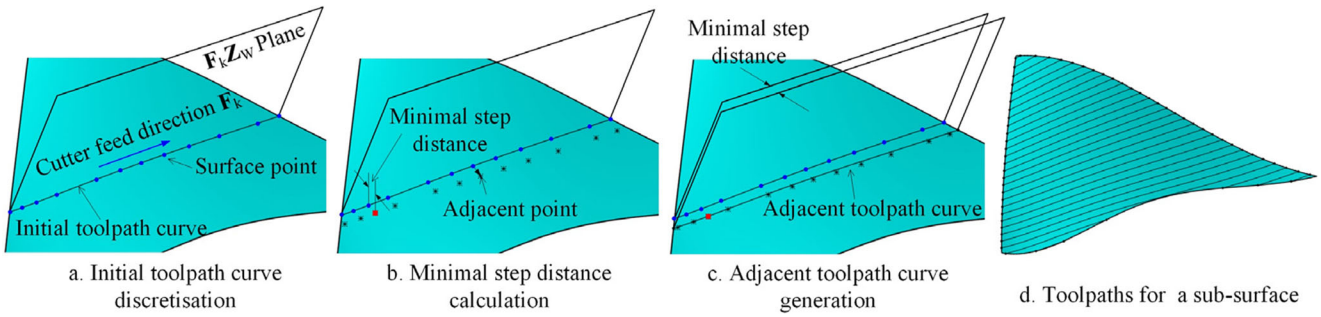

Fig. 13 Main procedures to generate toolpaths for a sub-surface. **a** Initial toolpath curve discretisation. **b** Minimal step distance calculation. **c** Adjacent toolpath curve generation. **d** Toolpaths for a sub-surface

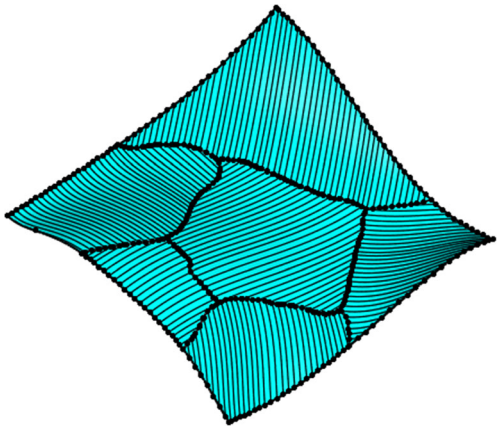

Fig. 14 3 + 2-axis machining toolpaths for the surface in Fig. 3

are obtained by discretizing $\boldsymbol{X}_W\boldsymbol{Y}_W$ across $\boldsymbol{O}_W$, as shown in Fig. 12. A list of two-tuples could be constructed as

$$\left\{\left(\boldsymbol{F}_{\mathrm{k}}, \boldsymbol{T}_{\mathrm{j}}\right) \middle| \boldsymbol{F}_{\mathrm{k}} \in \boldsymbol{F}, k \in [1\ \ \boldsymbol{F}.\mathrm{size}()]; \boldsymbol{T}_{\mathrm{j}} \in \boldsymbol{T}, \mathrm{j} \in [1\ \ \boldsymbol{T}.\mathrm{size}()]\right\} \quad (12)$$

where $\boldsymbol{T}$ only keeps the FTOs of the sub-surface. The $(\boldsymbol{F}_k, \boldsymbol{T}_j)$ leading to the maximal average MSW of the sub-surface will be selected for generating toolpaths.

At each surface point $\boldsymbol{P}_i$, the $\boldsymbol{X}_L$ of the LCS is parallel to $\boldsymbol{N}_i \times (\boldsymbol{F}_k \times \boldsymbol{N}_i)$. Then, λ_L and ω_L for describing $\boldsymbol{T}_j$ in LCS could be obtained. Points in ECP in Fig. 9d could be represented as

$$\mathrm{ECP}(\theta) = \begin{Bmatrix} 0 \\ r\cos\lambda_L \sin\omega_L \cos\theta - r\cos\lambda_L \cos\theta + r\cos\omega_L \sin\theta \\ -r\sin\lambda_L \cos\theta + r\sin\lambda_L \end{Bmatrix} \quad (13)$$

s' is the offset of sub-surface and the offset value equals to the maximal allowed cusp height δ. ECP intersect with s' at two positions: $\boldsymbol{I}_L$ and I_R. The distances between these two intersections and $\boldsymbol{P}_i$ in $\boldsymbol{Y}_L$ are w_L and w_R respectively. The MSW is w_L+w_R. $\boldsymbol{I}_L$ and $\boldsymbol{I}_R$ could be found by solving the following equation for θ:

$$D_1 \sin^2\theta + D_2 \sin\theta + D_3 \sin\theta\cos\theta - D_3 \cos\theta + D_4 = 0 \quad (14)$$

where

$$D_1 = \frac{r^2 \cos^2\lambda_L \sin^2\omega_L \kappa}{2}$$

$$D_2 = r\sin\lambda_L \cos\omega_L \sin\omega_L \kappa$$

$$D_3 = r^2 \cos\lambda_L \cos\omega_L \sin\omega_L \kappa$$

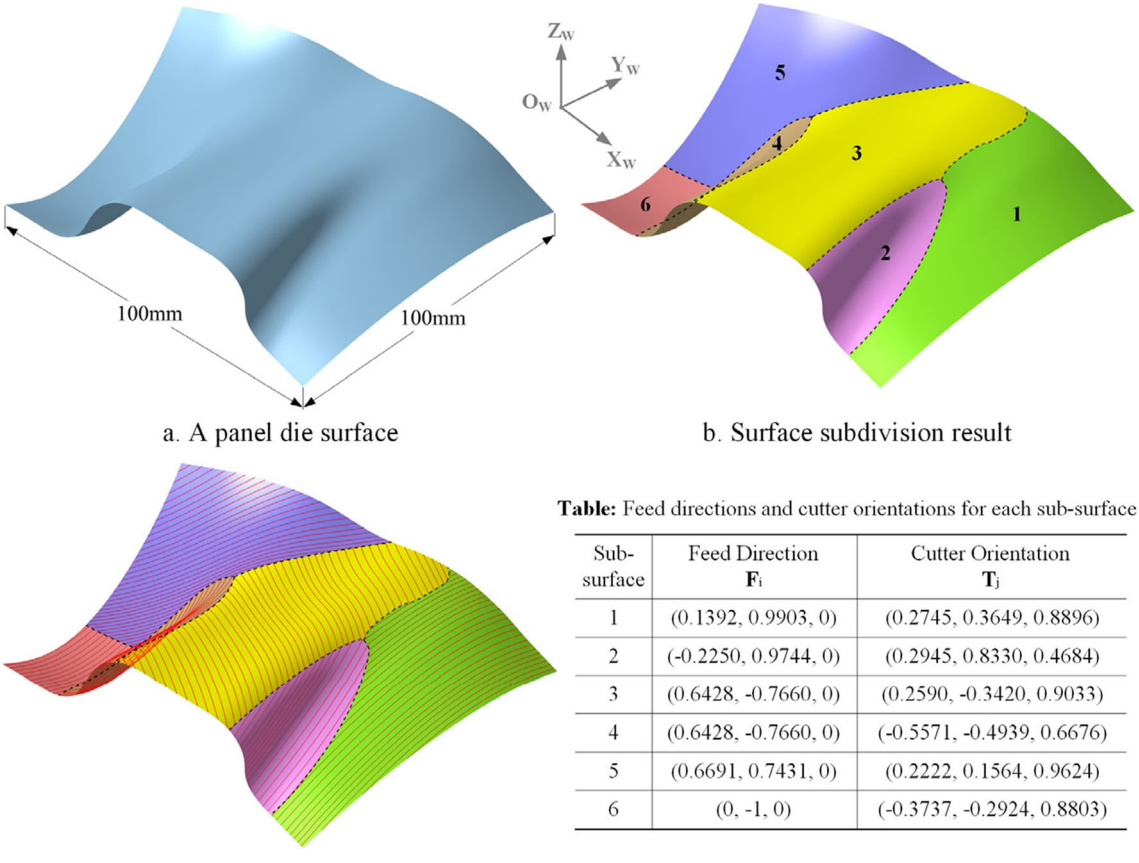

a. A panel die surface

b. Surface subdivision result

Table: Feed directions and cutter orientations for each sub-surface

Sub-surface	Feed Direction $\mathbf{F}_i$	Cutter Orientation $\mathbf{T}_j$
1	(0.1392, 0.9903, 0)	(0.2745, 0.3649, 0.8896)
2	(-0.2250, 0.9744, 0)	(0.2945, 0.8330, 0.4684)
3	(0.6428, -0.7660, 0)	(0.2590, -0.3420, 0.9033)
4	(0.6428, -0.7660, 0)	(-0.5571, -0.4939, 0.6676)
5	(0.6691, 0.7431, 0)	(0.2222, 0.1564, 0.9624)
6	(0, -1, 0)	(-0.3737, -0.2924, 0.8803)

c. Toolpaths for 3+2-axis machining

Fig. 15 Toolpaths generated by the proposed method. **a** A panel die surface. **b** Surface subdivision result. **c** Toolpaths for 3 + 2-axis machining

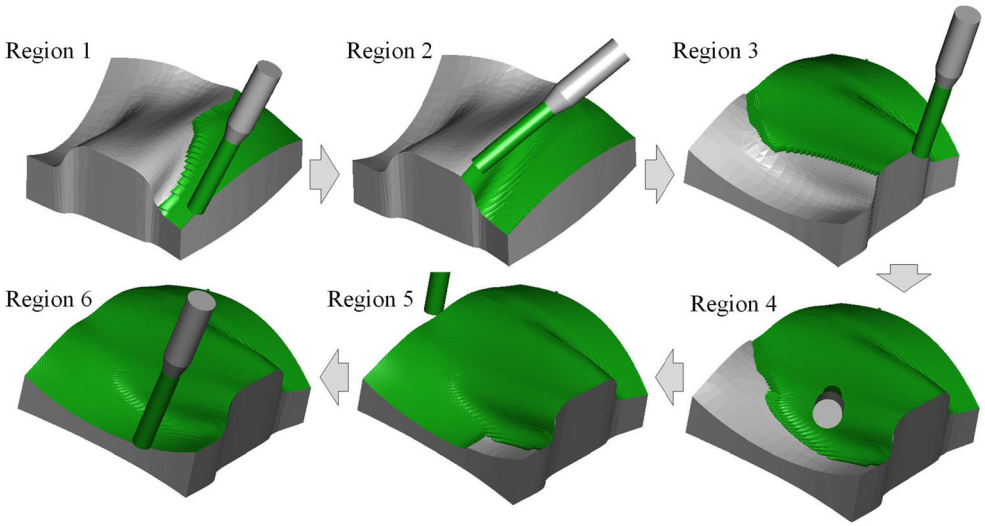

Fig. 16 Machining simulation with toolpaths generated by the proposed method

$$D_4 = \delta - r\sin\lambda_L + \frac{r^2\cos^2\lambda_L \sin^2\omega_L \kappa}{2}$$

where $\kappa = \kappa^{PS}_{Y_L Z_L}$. By finding θ_L and θ_R, $\boldsymbol{I}_L$ and $\boldsymbol{I}_R$ could be calculated; thus, MSW could be obtained. The average MSW of all sub-surface points with $(\boldsymbol{F}_k, \boldsymbol{T}_j)$ is

$$\mathrm{MSW_a} = \frac{\sum_{i=1}^{n} \mathrm{MSW_i}\left(\boldsymbol{F}_k, \boldsymbol{T}_j\right)}{n} \tag{15}$$

where $\mathrm{MSW_i}(\boldsymbol{F}_k, \boldsymbol{T}_j)$ is the MSW at $\boldsymbol{P}_i$ with $(\boldsymbol{F}_k, \boldsymbol{T}_j)$. $(\boldsymbol{F}_k, \boldsymbol{T}_j)$ that makes the maximal $\mathrm{MSW_a}$ will be selected.

For each sub-surface, create several planes that parallel to $\boldsymbol{F}_k\boldsymbol{Z}_W$ and intersect them with the sub-surface for potential initial toolpath curves. Discretise those curves into points and use the above method to calculate their MSWs. The curve with the maximal average MSW will be kept as the initial toolpath curve. To generate the adjacent toolpath is first to calculate the minimal step distance by applying the method proposed by Lee [24]. Then, move the plane corresponding to the current toolpath with this step distance to intersect the sub-surface for the next toolpath curve, as shown in Fig. 13.

With the above region-based 3 + 2-axis machining method, the toolpaths for surface mentioned in Fig. 3 could be calculated as shown in Fig. 14.

Table 1 Comparison results

Methods	Total toolpath length (mm)	Machining time
Proposed method	12,453.55	21 min 34 sec
3 + 2-axis machining	28,339.86	65 min 49 sec
5-axis machining	12,612.14	33 min 26 sec

4 Case study

The proposed method for generating region-based 3 + 2-axis machining toolpath is realised in the advanced machining module of CATIA V5 R19 by applying C++/MATLAB and CAA (Component Application Architecture) techniques. The surface shown in Fig. 15 is the scaling-down result of a panel die surface and is selected for testing the proposed method. The diameter of the flat end mill selected for finishing is 5 mm. The maximal allowed cusp height for finishing is 0.05 mm. DMU 80P duoBLOCK which is a B-C table-tilt type 5-axis machine is chosen. The rotation limits of axis B and C are [0° 180°] and [0° 360°] respectively. According to the proposed surface subdivision method, six sub-surfaces are acquired as shown in Fig. 15b. For each sub-surface, the feed direction and the cutter orientation in WCS which leads to the maximal average MSW of points within the sub-surface is calculated for generating toolpaths as shown in Fig. 15c and the simulation result could be found in Fig. 16. For this test surface, finishing toolpaths are also generated using two existing traditional methods for comparison. Real machining tests are also carried out to compare the finishing time as

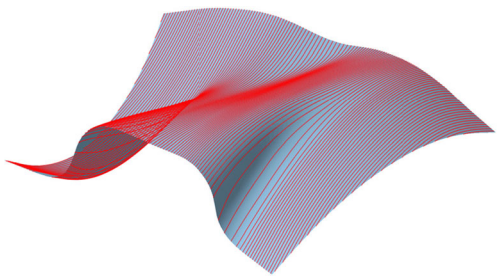

Fig. 17 3 + 2-axis machining toolpaths for the whole surface

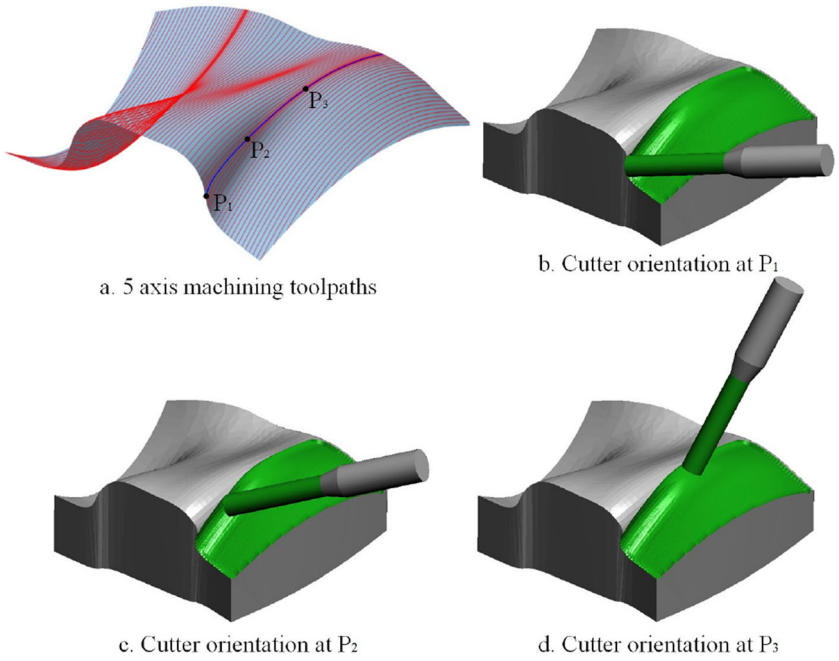

Fig. 18 5-axis machining toolpaths. **a** 5-axis machining toolpaths. **b** Cutter orientation at P_1. **c** Cutter orientation at P_2. **d** Cutter orientation at P_3

shown in Fig. 19 and the feed speeds are all assigned to 1000 mm/min. From Table 1, it could be found that using the proposed method to machine the test surface could get a better result both in total toolpath length and machining time.

In traditional 3 + 2-axis machining, the whole surface is usually machined with one fixed tool orientation as shown in Fig. 17. However, since the geometry of surfaces become much more complicated, there are few FTOs which are gouging and collision free to all surface points. As a result, it is difficult or even impossible to determine the fixed cutter orientation. Even though an admissible tool orientation could be found, there is a great probability to result in small MSWs which will further lead to dense toolpaths. The consequence is both the total toolpath length and the machining time is longer than the proposed method.

Figure 18a shows the 5-axis machining toolpaths generated by the multi-axis sweeping function of CATIA. The yaw angle is fixed to 0° while the tilt angle varies during machining. It is known that when machining complex surfaces, 5-axis machining toolpaths usually result in great changes to the tool orientations, as shown in Fig. 18b–d. For most 5-axis machine tools, like the selected DMU 80P duoBLOCK, the kinematic capabilities of rotary axes B and C are much weaker than that of its linear axes X, Y and Z. As a result, though the total toolpath length is much shorter than the traditional 3 + 2-axis machining, the machining time reduction is not as good as shown in Table 1. The machined surface in Fig. 19 is measured and the result shows that no overcut happened and the maximal allowed cusp height of 0.05 mm is also satisfied.

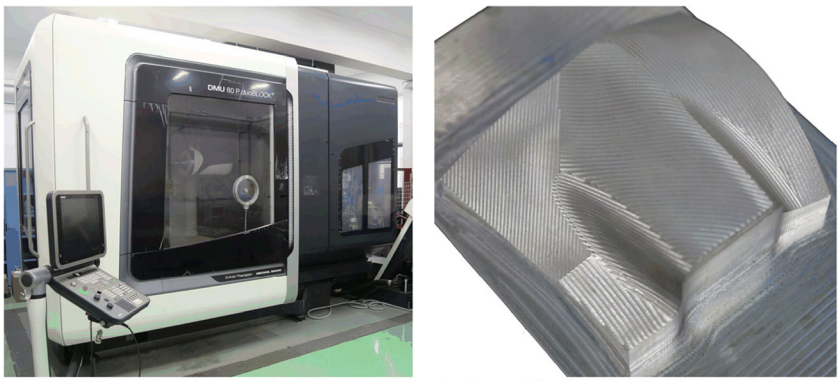

Fig. 19 Test surface machining using the proposed method. **a** The machine tool used to machine the test surface. **b** The machined result using the proposed method

5 Conclusions

During the 5-axis machining of some complex surfaces, tool orientations usually change greatly for gouging and collision avoidance. Since for most 5-axis machine tools, the kinematic capabilities of rotary axes are much weaker than that of the linear axes; how to improve the machining efficiency becomes an urgent issue in traditional 5-axis machining. This paper focuses on a special tool orientation strategy named 3 + 2-axis which uses the 5-axis capability to orient the tool and fixes this tool orientation during the machining. This strategy is able to increase the real feed speed since the rotary axes keep static during machining. The difficulty is the determination of this fixed tool orientation. Local gouging, rear gouging and global collision should be avoided; the feasible tool orientations are limited or even non-existent. This paper proposed a region-based 3 + 2-axis machining toolpath generation method. The surface is divided into several preliminary sub-surfaces by applying K-means clustering algorithm at the first stage. To ensure the surface quality, a post processing procedure is put forward by partitioning and merging the areas with bad machinability to optimise the subdivision result. For each sub-surface, gouging-/collision-free tool orientations are first calculated and then the optimal combination of the fixed tool orientation and the feed direction is determined by maximising the average MSW of all surface points to generate toolpaths. With this method, each sub-surface could be machined using the fixed tool orientation determined by only considering its local geometry which means closer match of the cutter's shape to the surface. Thus, the toolpath length as well as the machining time could be much shorter than that of the traditional 3 + 2-axis and 5-axis machining method. A surface is chosen to test the proposed method and the comparisons to traditional 3 + 2-axis and 5-axis machining methods are also provided. The result shows the proposed method is better in both total toolpath length and machining time. In the future work, efforts will be made for improving the computation efficiency and the machining quality around the inside boundaries.

Funding information The results presented in this paper are generated from the projects funded by National Natural Science Foundation Project of China (No. 51605217 and U1537209) and the Jiangsu Province Outstanding Youth Fund (No. BK20140036).

Publisher's Note Springer Nature remains neutral with regard to jurisdictional claims in published maps and institutional affiliations.

References

1. Li YG, Lee ZH, Gao J (2015) From computer-aided to intelligent machining: recent advances in CNC machining research. Proc Inst Mech Eng B J Eng Manuf 229(7):1087–1103
2. Lasemi A, Xue DY, Gu PH (2010) Recent development in CNC machining of freeform surfaces: a state-of-the-art review. Comput Aided Des 42(7):549–566
3. Zhang K, Tang K (2016) Optimal five-axis tool path generation algorithm based on double scalar fields for freeform surfaces. Int J Adv Manuf Technol 83(9–12):1503–1514
4. Wang Y, Yan CY, Yang JZ, LEE CH (2017) Tool path generation algorithm based on covariant field theory and cost functional optimization and its applications in blade machining. Int J Adv Manuf Technol 90(1–4):927–943
5. Jun CS, Cha K, Lee YS (2003) Optimizing tool orientation for 5-axis machining by configuration-space search method. Comput Aided Des 35(6):641–654
6. Lu J, Cheatham R, Jensen CG, Chen Y, Bowman B (2008) A three-dimensional configuration-space method for 5-axis tessellated surface machining. Int J Comput Integr Manuf 21(5):550–568
7. Wang N, Tang K (2007) Automatic generation of gouge-free and angular-velocity-compliant five-axis toolpath. Comput Aided Des 39(10):841–852
8. Castagnetti C, Duc E, Ray P (2008) The domain of admissible orientation concept: a new method for five-axis toolpath optimization. Comput Aided Des 40(9):938–950
9. Farouki RT, Li SQ (2013) Optimal tool orientation control for 5-axis CNC milling with ball-end cutters. Comp Aided Geom Des 30(2):226–239
10. Lee YS, Ji H (1997) Surface interrogation and machining strip evaluation for 5-axis CNC die and mold machining. Int J Prod Res 35(1):225–252
11. Fard MJB, Feng HY (2009) Effect of tool tilt angle on machining strip width in five-axis flat-end milling of free-form surfaces. Int J Adv Manuf Technol 44(3–4):211–222
12. Gong H, Fang FZ, Hu XT, Cao LX, Liu J (2010) Optimization of tool positions locally based on the BCELTP for 5-axis machining of free-form surfaces. Comput Aided Des 42(6):558–570
13. Liu X, Li YG, Gao J (2015) A multi-perspective dynamic feature concept in adaptive NC machining of complex freeform surfaces. Int J Adv Manuf Technol 82(5):1259–1268
14. Chiou CJ, Lee YS (2002) A machining potential field approach to toolpath generation for multi-axis sculptured surface machining. Comput Aided Des 34(5):357–371
15. Anotaipaiboon W, Makhanov SS (2005) Toolpath generation for five-axis NC machining using adaptive space-filling curves. Int J Prod Res 43(8):1643–1665
16. Liu X, Li YG, Ma SB, Lee CH (2015) A toolpath generation method for freeform surface machining by introducing the tensor property of machining strip width. Comput Aided Des 66:1–13
17. Gray JP, Ismail F, Bedi S (2007) Arc-intersect method for $3\frac{1}{2}\frac{1}{2}$-axis toolpaths on a 5-axis machine. Int J Machine Tools Manuf 47(1):182–190
18. Chen ZC, Dong ZM, Vickers GW (2003) Automated surface subdivision and toolpath generation for $3\frac{1}{2}\frac{1}{2}$-axis CNC machining of sculptured parts. Comp Ind 50(3):319–331
19. Roman A, Bedi S, Ismail F (2006) Three-half and half-axis patch-by-patch NC machining of sculptured surfaces. Int J Adv Manuf Technol 29(5):524–531

20. Flores RA (2007) Surface partitioning for 3+2-axis machining. University of Waterloo, Waterloo, ON, Canada
21. Bi Q, Ding H, Wang Y. Safe and short tool length generation for 3+2 axis NC machining of a ball-end cutter using graphics hardware. In: Xiong C, et al., editors. Intelligent robotics and applications. ICIRA 2008: Proceedings of the first international conference on intelligent robotics and applications; 2008 Oct 15–17; Wuhan, China. Berlin: Springer; 2008: 348–355
22. Zhu Y, Chen ZT, Ning T, Xu RF (2016) Tool orientation optimization for 3+2-axis CNC machining of sculptured surface. Comput Aided Des 77:60–72
23. Lee YS (1998) Mathematical modelling using different endmills and tool placement problems for 4- and 5-axis NC complex surface machining. Int J Prod Res 36(3):785–814
24. Lee YS (1998) Non-isoparametric toolpath planning by machining strip evaluation for 5-axis sculptured surface machining. Comput Aided Des 30(7):559–570